



Inverse optimization of hydraulic, solute transport, and cation exchange parameters using HP1 and UCODE to simulate cation exchange

Diederik Jacques^{a,*}, Chris Smith^b, Jiří Šimůnek^c, David Smiles^b

^a Institute for Environment, Health, and Safety, Belgian Nuclear Research Centre (SCK•CEN), Mol, Belgium

^b CSIRO Land and Water, Canberra, ACT, Australia

^c University of California Riverside, Riverside, CA, USA

ARTICLE INFO

Article history:

Received 21 November 2011

Received in revised form 15 March 2012

Accepted 30 March 2012

Available online 5 April 2012

Keywords:

Fertilization

Coupled reactive transport

Unsaturated water flow

Calibration

ABSTRACT

Reactive transport modeling is a powerful tool to evaluate systems with complex geochemical relations. However, parameters are not always directly measurable. This study represents one of the first attempts to obtain hydrologic, transport and geochemical parameters from an experimental dataset involving transient unsaturated water flow and solute transport, using an automatic inverse optimization (or calibration) algorithm. The data come from previously published, controlled laboratory experiments on the transport of major cations (Na, K, Mg, Ca) during water absorption into horizontal soil columns that were terminated at different times. Experimental data consisted of the depth profiles of water contents (θ), Cl concentrations, and total aqueous and sorbed concentrations of major cations. The dataset was used to optimize several parameters using the reactive transport model, HP1 and the generic optimization code, UCODE. Although the soil hydraulic and solute transport parameters were also optimized, the study focused mainly on the geochemical parameters because the soil columns were constructed from disturbed soil. The cation exchange capacity and the cation exchange coefficients for two exchange models (Gapon and Rothmund–Kornfeld) were optimized. The results suggest that both calibrated models satisfactorily described the experimental data, although the Rothmund–Kornfeld model fit was slightly better. However, information content and surface response analyses indicated that parameters of the Gapon model are well identifiable, whereas those of the Rothmund–Kornfeld model were strongly correlated. The calibrated geochemical parameters were validated using an independent dataset. In agreement with the identifiability analysis, the Gapon approach was better than the Rothmund–Kornfeld model at calculating the observed concentrations of major cations in the soil solution and on the exchange sites.

© 2012 Elsevier B.V. All rights reserved.

1. Introduction

Various human activities, such as irrigation of agricultural lands, may alter the geochemistry of soil systems (e.g. Gonçalves et al., 2006; Ramos et al., 2011). In this study, we evaluate data collected for the analysis of the wet flush system for intensive piggeries. Such systems produce large

volumes of effluent from the urine, feces and waste feed. In Australia, irrigation with treated effluent is the most productive way to utilize this waste product. In addition to high nutrient content, the effluents also contain high concentrations of K and Na (Smiles and Smith, 2004a,b). Potassium is becoming the dominant monovalent ion released into the environment, as piggery operators, concerned about the effects of Na on soil properties, have replaced Na with K salts in the feed. The use of the K-rich effluent for irrigation has increased K concentrations in the soil solution and on the cation exchange sites (Smiles and Smith, 2004a).

* Corresponding author.

E-mail address: DJACQUES@SCKCEN.BE (D. Jacques).

In principle, the fate of cations in solution and sorbed by soils under natural conditions can be predicted using models that simulate variably-saturated water flow and solute transport, while considering reaction chemistry and/or chromatographic theory. Examples are LEACHM (Hutson and Wagenet, 1992) and/or HP1 (Jacques et al., 2006), which couples HYDRUS-1D (Šimůnek et al., 2008a) with PHREEQC (Parkhurst and Appelo, 1999). However, the use of such complex numerical models requires specification of a large number of soil hydraulic, solute transport, and biogeochemical reaction input parameters. In the application involving irrigation with piggery effluent, cation exchange parameters are of particular interest. Several approaches exist to obtain these parameters. For example, the competitive exchange of Na, K, and Ca during absorption by initially homoionic soils was studied by Bond and Phillips (1990a,b), Bond (1997), and Bond and Verburg (1997). In other studies, cation exchange parameters were estimated or calibrated using detailed information on binary sorption isotherms and then applied to ternary (or multication) transport experiments (e.g., Voegelin et al., 2000, 2001; Vulava et al., 2000). Alternately, Appelo and Postma (2005; pages 252–260) outlined an approach in which cation exchange can be modeled without the need of prior knowledge of the adsorption isotherms for each pair of competing cations in the presence of all the others.

In this study, we propose to obtain flow, transport, and geochemical parameters by calibrating an appropriate model against experimental data involving reactive transport under unsaturated transient conditions in natural soils. Suitable datasets for such analysis are rarely available (e.g., Mansell et al., 1993). The experimental data of Smiles and Smith (2004b), involving water absorption with piggery effluent into initially unsaturated soil columns, provided detailed profiles of water contents and aqueous and sorbed concentrations. This dataset gives us the opportunity to investigate the use of inverse optimization to estimate geochemical parameters.

The use of parameter estimation techniques is well-established for determining soil hydraulic properties (e.g., Hopmans et al., 2002; Vrugt et al., 2008) or basic solute transport and reaction parameters (e.g., Šimůnek et al., 2002, 2008b; and references given there). This approach has been widely used for various laboratory and field experiments. Estimation of soil hydraulic properties typically requires transient, variably-saturated flow experiments and numerical models such as HYDRUS-1D. On the other hand, solute transport parameters are often derived from column experiments under steady-state water flow conditions (e.g., Nkedi-Kizza et al., 1984). Analytical solutions of the transport equations are then fitted to experimental breakthrough curves by using parameter estimation codes such as CXTFIT (Toride et al., 1995) or STANMOD (Šimůnek et al., 2008b). Obtaining solute transport parameters for conditions for which no analytical solutions exist, such as for transient flow conditions and/or nonlinear biogeochemical reactions such as adsorption or cation exchange, can be accomplished only using numerical solutions (Dai and Samper, 2004; Šimůnek et al., 2002, 2008b).

The current study represents one of the first attempts to obtain soil hydrologic, transport, and geochemical parameters with an automatic inverse optimization algorithm and experimental data obtained under transient water flow

conditions. This is accomplished using the universal optimization code UCODE (Poeter et al., 2005) with the numerical model HP1. The previously acquired experimental dataset of Smiles and Smith (2004b) is used to calibrate: i) the soil hydraulic parameters of the van Genuchten–Mualem model (van Genuchten, 1980); ii) the solute transport parameters (dispersivity); and, most importantly, iii) the geochemical parameters (major cation exchange coefficients). The identifiability of the cation exchange parameters is investigated for the presented experimental setup by analyzing parameter sensitivities and response surfaces.

2. Material and methods

2.1. Experimental setup

Two laboratory experimental datasets were used in this study. In the first set of experiments, soil columns were placed in contact with an artificial piggery effluent (Smiles and Smith, 2004b). Because of the destructive nature of utilized methods, three soil columns were prepared to measure concentration profiles at three different times. Data collected at these three columns were used to calibrate flow, transport, and exchange parameters. The second dataset was obtained from a series of experiments, in which two soil columns were placed in contact with gypsum-saturated solutions (Smiles and Smith, 2008). This dataset was used to validate optimized parameters.

Details of the method used to produce the first dataset are given in Smiles and Smith (2004b). In brief, the topsoil (0–100 mm) from a Deep Red Chromosol [site 5 of Smiles and Smith, 2004a] was used. The soil had not previously been irrigated with piggery effluent. The soil contains 15–20% clay (by mass) and has a cation exchange capacity (CEC) of 46 mmol_c/kg. This is equal to a CEC value of $0.077 \pm 0.002 \text{ mol}_c/\text{dm}^3$, providing the average soil bulk density was $1.68 \pm 0.05 \text{ kg}/\text{dm}^3$. More information on the soil is given in Smiles and Smith (2004a).

In the first set of laboratory experiments, sieved soil (<2-mm) with a water content (θ_v) of $\approx 0.05 \text{ g/g}$ was packed into acrylic columns with a 20-mm internal diameter and 20 cm long. The columns were made from sections 4, 6, and 10 mm long with the shortest sections close to the inflow end. The soil was added in increments of 2–3 g and packed using a small drop hammer to ensure uniformity. The resulting soil bulk density was $1.68 \pm 0.05 \text{ kg}/\text{dm}^3$ throughout the column. A solution with a cation composition similar to piggery effluent, but with Cl^- as the sole anion, was applied at zero water potential to one end of the horizontal column. The artificial effluent had the following composition: Na = 10 mmol_c/L; K = 20.1 mmol_c/L; Ca = 4.69 mmol_c/L, and Cl = 35 mmol_c/L (Smiles and Smith, 2004b). The pH of the artificial effluent was 7.7. Initial pore water concentrations in the columns were: Na = 5 mmol_c/L, K = 2 mmol_c/L, Ca = 40 mmol_c/L, Mg = 8 mmol_c/L, and Cl = 4 mmol_c/L.

The experiments were terminated by sectioning the columns after 36, 106, and 144 min. Each moist section was weighed and a water sample was removed by centrifuging in the presence of 5 cm³ of 1,1,2-trichloro-1,2,2-trifluoro ethane that had a specific gravity of 1.57 (Phillips and Bond, 1989). The soil sample was washed with glycerated alcohol to

remove excess water-soluble cations, and then exchangeable cations were extracted with 1 M NH_4Cl . After washing with alcohol, the CEC was estimated by measuring the remaining NH_4^+ (Rayment and Higginson, 1992).

Water-soluble cations were measured by inductively coupled plasma spectroscopy (ICP) of the water sample after diluting a small volume of soil solution ($0.2\text{--}0.5\text{ cm}^3$) to 10 cm^3 . Exchangeable cations were measured in the NH_4Cl extract by atomic absorption spectroscopy (AAS). The NH_4^+ representing the exchange capacity was measured using an autoanalyser (Rayment and Higginson, 1992). Dilutions were tracked gravimetrically and all quantities were referred to the oven-dry weight of soil in each section, which was measured by oven drying following all extractions.

The second dataset is from Smiles and Smith (2008). Briefly, the acrylic columns used in the first series of experiment were packed with potassic soil to a bulk density of $1.76 \pm 0.2\text{ kg/dm}^3$. This soil was the same as the one used to develop the optimized geochemical parameters, except that it had been irrigated with K-rich piggery effluent and thus had a high exchangeable K ratio. A gypsum-saturated solution was then applied at one end of the horizontal columns from a Mariotte bottle set at a small suction ($\sim 5\text{ mm}$), and the experiments were terminated after 200 and 400 min. The gypsum solution consisted of 24 mmol/L of Ca and 24 mmol/L of S(6). The initial soil solution concentrations were: 28 mmol/L of Na, 30 mmol/L of K, 40 mmol/L of Ca, 9 mmol/L , and 13 mmol/L of Cl. The experimental methods were the same as in the first set of experiments.

2.2. Model description

Modeling the transport of major cations through the soil cores involves modeling the following processes: a) water flow; b) solute transport (advection and dispersion); and c) geochemical reactions (aqueous complexation and cation exchange).

Water absorption is modeled using a numerical solution of the Richards equation, which requires knowledge of the water retention curve (the relation between the water content θ [$\text{cm}^3\text{ cm}^{-3}$] and the pressure head h [cm]), and the unsaturated hydraulic conductivity function (the relation between the hydraulic conductivity K [cm min^{-1}] and the pressure head). These nonlinear relations are parameterized using the closed-form system of equations proposed by van Genuchten (1980):

$$\theta(h) = \theta_r + \frac{\theta_s - \theta_r}{(1 + |\alpha h|^m)^{1/m}} \quad (1)$$

$$K(h) = K_s S_e^l \left[1 - \left(1 - S_e^{1/m} \right)^m \right]^2 \quad (2)$$

These equations have six adjustable parameters: the saturated water content θ_s [$\text{cm}^3\text{ cm}^{-3}$], the residual water content θ_r [$\text{cm}^3\text{ cm}^{-3}$], two shape parameters α [cm^{-1}] and n [–], the saturated hydraulic conductivity K_s [cm min^{-1}], and a pore-connectivity and tortuosity factor l [–]. The degree of

saturation S_e and the parameter m are obtained from the other parameters: $S_e = (\theta - \theta_r)/(\theta_s - \theta_r)$ and $m = 1 - 1/n$.

Transport of the aqueous components (that is, the total aqueous concentration of an element) is described with the advection–dispersion equation:

$$\frac{\partial \theta C_i}{\partial t} = \frac{\partial}{\partial x} \left(\theta D^w \frac{\partial C_i}{\partial x} \right) - \frac{\partial q C_i}{\partial x} + R_i \quad (3)$$

where t is time [min], x is spatial distance [cm], i ($= 1, \dots, N_m$) is the aqueous component number (N_m is the total number of aqueous components), C_i is the total aqueous concentration of the i th component [mol cm^{-3}], q is the volumetric flux density [cm min^{-1}], D^w is the dispersion coefficient in the liquid phase [$\text{cm}^2\text{ min}^{-1}$], and R_i is the general source/sink term due to geochemical reactions [$\text{cm cm}^{-3}\text{ min}^{-1}$]. In general, this sink/source term (R_i) contains heterogeneous (between different phases) equilibrium reactions and homogeneous (within one phase) and heterogeneous kinetic reactions. In the current study, only heterogeneous equilibrium reactions are accounted for. The dispersion coefficient is defined as:

$$\theta D^w = \lambda |q| + \theta D^{w0} \tau_w \quad (4)$$

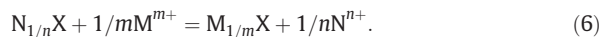
where D^{w0} is the molecular diffusion of aqueous components in free water [$\text{cm}^2\text{ min}^{-1}$], λ is the longitudinal dispersivity [cm], and τ_w is a tortuosity factor in the liquid phase [–], calculated using the model of Millington and Quirk (1961):

$$\tau_w = \frac{\theta^{7/3}}{\theta_s^2} \quad (5)$$

In the multicomponent transport model described above (Eqs. (3)–(5)), only one unknown transport parameter (i.e., the dispersivity, λ) is needed to characterize the flow field.

Two geochemical processes were considered in the current study: aqueous speciation reactions and cation exchange. The former is described by a set of aqueous complexation reactions and corresponding mass action constants. The *phreeqc.dat* database (Parkhurst and Appelo, 1999) is used for the aqueous complexation reactions, the mass action constants, and activity correction models.

The relation between the concentrations of ions in the pore water and on the surface exchange sites may be described using the Gapon convention (Appelo and Postma, 2005). The equation of the exchange reaction on surface site X, involving cations N and M , with charges of n and m respectively, is:

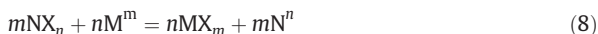


The selectivity coefficient K_{GMN} is given:

$$K_{GMN} = \frac{[M_{1/m}X][N^{n+}]^{1/n}}{[N_{1/n}X][M^{m+}]^{1/m}} \quad (7)$$

where the square brackets [] represent activities. The activity of each exchangeable species is equal to its equivalent fraction. Here the subscript G refers to the Gapon formulation.

An alternative exchange convention is the Rothmund–Kornfeld equation (Bloom and Mansell, 2001; Bond, 1995). For exchange reactions written as:



the selectivity coefficient, K_{RKMN} , is defined as:

$$K_{RKMN} = \frac{[MX_m]^n}{[NX_n]^m} \left(\frac{[N^n]^m}{[M^m]^n} \right)^{N_{MN}} \quad (9)$$

where N_{MN} is an empirical exponent for the activity ratio of the aqueous species. This exponent enables the model to describe sigmoidal shapes of binary isotherms, which reflect the sorption of species to strong-binding sites when concentrations of one of the species is low (Appelo and Postma, 2005).

2.3. Simulation tool

The HP1 code (Jacques et al., 2006, 2008a,b; Šimůnek et al., 2006, 2009) was used as the simulator to solve the coupled flow, transport, and geochemical problem. HP1 (version 2.3) couples the water flow, multiple solute transport and heat transport code HYDRUS-1D (Šimůnek et al., 2008a) with the geochemical equilibrium and kinetic code PHREEQC (version 2.17.5) (Parkhurst and Appelo, 1999). The transport simulator solves the water flow and solute transport equations, whereas the geochemical simulator calculates chemical speciation in the aqueous phase and on the exchange complexes.

The Gapon exchange reactions are defined as half reactions ($X^- + 1/m M^{m+} = M_{1/m}X$ with a thermodynamic constant K_{GM}) relative to a reference half reaction (in PHREEQC; the half reaction with Na has $\log K_{GN} = 0$). Note that each Gapon exchange reaction (Eq. (6)) can be written as a linear combination of the defined half reactions (given in Appendix 1). As such, the thermodynamic constants of the half reactions for the other cations are related to the Gapon selectivity coefficient as $\log K_{GMN} = \log K_{GM} - \log K_{GN}$. The Rothmund–Kornfeld equation is implemented following example 6.6 in Appelo and Postma (2005) (see also Appendix 1).

2.4. Inverse optimization

Unknown parameters of the described model are: θ_s , θ_r , α , n , K_s , l , λ , K_{GK} , K_{GCa} , K_{GMg} , and CEC for the Gapon approach; and θ_s , θ_r , α , n , K_s , l , λ , K_{RKKNa} , K_{RKCNa} , K_{RKMgNa} , N_{KNa} , N_{CaNa} , N_{MgNa} and CEC for the Rothmund–Kornfeld approach. These parameters are estimated using the measured profiles of water contents, Cl concentrations, aqueous Na, K, Ca, and Mg concentrations, and sorbed Na, K, Ca, and Mg concentrations, by minimizing the sum of squared differences between observations and corresponding simulated values.

A sequential parameter estimation procedure is used here. HYDRUS-1D alone is used first to estimate the soil hydraulic and solute transport parameters because the flow and transport simulator of HP1 is essentially identical to the HYDRUS-1D code. The inverse optimization algorithm based on the Levenberg–Marquardt nonlinear minimization method

(Marquardt, 1963) embedded within HYDRUS-1D is used for this purpose. In the next step, the geochemical parameters are estimated by HP1 using the model-independent optimization tool, UCODE (Poeter et al., 2005). The objective function is obtained as a weighted sum of squared differences (SSD) between observations and experimental data. Weights are defined to minimize differences in weighting between different data types (Clausnitzer and Hopmans, 1995):

$$w_j = \frac{1}{n_j \sigma_j} \quad (10)$$

where w_j is the weight for the j th data point, n_j is the number of observations for a given data type and σ_j is the measurement variance within a given data type. Twenty four different data types are used when optimizing cation exchange parameters: aqueous and sorbed concentration profiles of four cations at three times.

The initial and boundary conditions used in the modeling exercise were as follows: the initial volumetric water content was $0.084 \text{ cm}^3 \text{ cm}^{-3}$, the volumetric water content at the inlet of the column was set to $0.305 \text{ cm}^3 \text{ cm}^{-3}$ (inferred from the experimental data close to the inlet end of the horizontal column), and the outlet boundary was set to free drainage. The initial estimate of CEC of the soil was 0.085 mol/dm^3 . In this particular example, the initial estimate of CEC is not critical since this parameter is well-defined, as discussed below in the section “Response surface analysis of the objective function”. Cation exchange capacity was optimized since the bulk density (and thus CEC) varied slightly within and between soil columns. One additional optimization was also carried out without fitting CEC to evaluate if the use of the measured CEC has an effect on fitted selectivity coefficients. The initial estimates of the Gapon selective coefficients for Ca/Na, Ca/K, and Ca/Mg exchange were $K_{GCaNa} = 2.9$, $K_{GCaK} = 0.2$, and $K_{GCaMg} = 1.2$ respectively, as the middle values of the ranges given in MDH (2003). Because of the lack of additional information, the same initial values were also used for the Rothmund–Kornfeld selectivity coefficients and n was initially set at 0.7, 0.9 and 0.9 for n_{KNa} , n_{CaNa} , and n_{MgNa} , respectively.

It is important to emphasize that the hydraulic and solute transport parameters are fitted only to reproduce the water flow and solute transport conditions so that the reactive constants could be determined from these transient experiments. Because the experiments were done for disturbed soils, these parameters may not be representative of undisturbed soil conditions. As such, uniqueness and correlation between the hydraulic and transport parameters (see parameter identifiability) are not further assessed here. The reader is referred to other studies on identifiability of hydraulic and transport parameters (e.g., Šimůnek and van Genuchten, 1996; Toorman et al., 1992).

2.5. Parameter identifiability

Identification of parameters using an inverse optimization approach requires that there is enough information in the experimental data to obtain unique and/or well-defined parameters. Two types of analysis were performed in order to investigate the identifiability of the cation exchange parameters in this particular experimental set up. The first

analysis uses dimensionless and composite scaled sensitivities. The dimensionless scaled sensitivity of the i th observation and j th parameter, dss_{ji} , is defined as (Hill and Tiedeman, 2007):

$$dss_{ji} = \left(\frac{\partial y_j}{\partial b_i} \right) \Big|_b |b_i| w_j^{1/2} \quad (11)$$

where y_j is the simulated value corresponding to a given observation, b_i is the i th estimated parameter, \mathbf{b} is the vector, which contains the parameter values at which the sensitivities are evaluated, and w_j is the weight of the j th observation point as defined above. The sensitivity is the derivative of the simulated value with respect to the parameter b_i . It provides information on the relative importance of an observation to the estimation of a single parameter, compared to the other observations. Larger values of dss_{ji} indicate observations containing more information. Alternatively, the dimensionless scaled sensitivity also provides a measure that compares the relative importance of a given parameter for a given simulated value. The information content of different sets of data types is quantified by taking the sum of the absolute values of the dimensionless scaled sensitivities. The average value is used to compare the different data types (e.g., profiles at a given time of the aqueous or sorbed concentrations, or the sum of the three profiles for a given aqueous or sorbed species).

The composite-scaled sensitivity for the i th parameter (css_i) is calculated as (Hill and Tiedeman, 2007):

$$css_i = \sum_{j=1}^{N_{obs}} \left[\left(dss_{ji} \right)^2 \Big|_b / N_{obs} \right]^{1/2} \quad (12)$$

where N_{obs} is the number of observations.

The composite-scaled sensitivity provides a means to evaluate the amount of information in all experimental data to estimate a given parameter. For example, Friedel (2005) interpreted css for different combinations of data types in a coupled water–heat–solute transport model.

The second analysis is based on the evaluation of response surfaces (e.g., Šimůnek and van Genuchten, 1996; Toorman et al., 1992). A response surface is a two-dimensional plot of the objective function obtained by varying two parameters, usually on a regular grid (80×80 in this study), while keeping the other parameters at their fitted values. Since only the cation exchange parameters are included in this analysis, there are 6 contour plots for the Gapon approach and 21 plots for the Rothmund–Kornfeld approach.

3. Result and discussion

Experimental data from Smiles and Smith (2004b) are presented in Fig. 1 (water contents and chloride concentrations) and in Fig. 2 (aqueous and sorbed cation concentrations). Note that due to the large scatter in the 36-minute K and Cl concentrations (attributed to the contamination of soil samples), these data were discarded from the fitting procedure. The data are plotted as a function of the Boltzmann variable (distance/time^{0.5}) because, for the given boundary conditions, water content and ion concentration

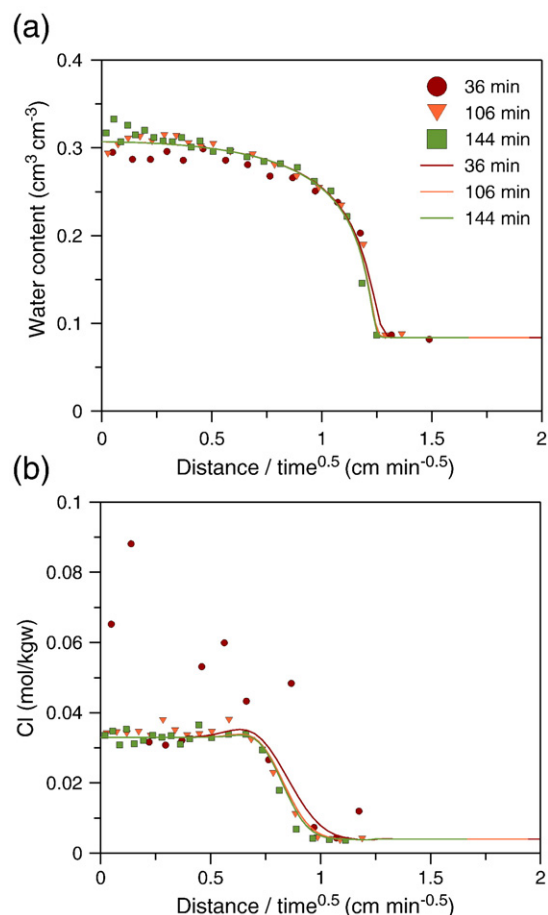


Fig. 1. Simulated [lines] profiles of water contents (a) and chloride concentrations (b) compared to experimental data [symbols] from water absorption and solute transport experiments with piggy effluent (Smiles and Smith, 2004b).

profiles should coalesce to a single curve when graphed in terms of the Boltzmann variable (Smiles and Smith, 2004b). For a full interpretation of the experimental dataset, the reader is referred to that study. Only the key findings are listed below in order to facilitate interpretation of modeled experimental results. The piston front (the location in the column where the infiltrating solution completely displaces the initial water) is between 0.75 and 0.85 cm/min^{0.5} (see Smiles and Smith, 2004b). Non-reactive solutes (such as Cl) should have the center of their diffusive front around this location (Fig. 1b). A change in aqueous concentrations of the reactive cations (Mg and Ca in Fig. 2c and d) around the piston front occurs without any noticeable change in sorbed concentrations. This is because of the concentration differences between the initial solution (the total sum of cations is about 35 mmol_c/L) and the infiltrating solution (the total sum of cations is about 60 mmol_c/L). Across the piston front, the cation ratios are buffered by the exchange processes so that the total concentration adjusts while the sorbed and aqueous cation ratios appear to stay constant. Concentration changes around the piston front are thus associated with the

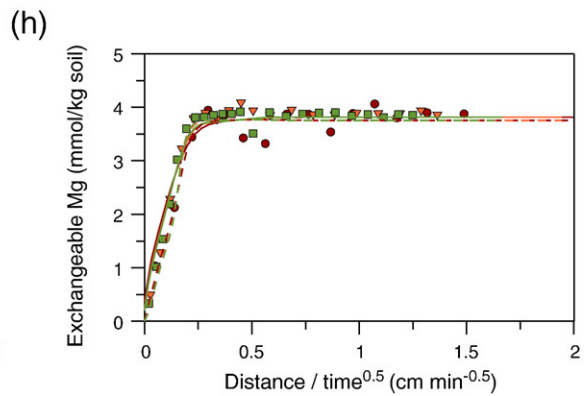
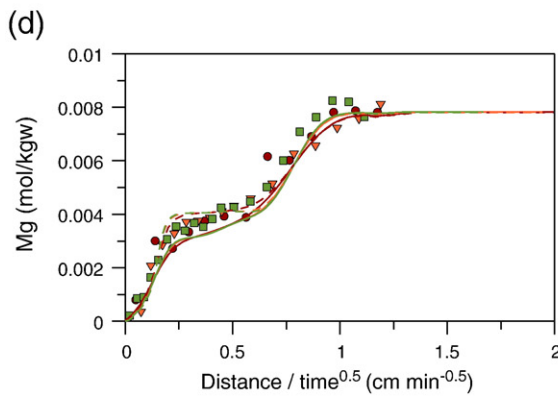
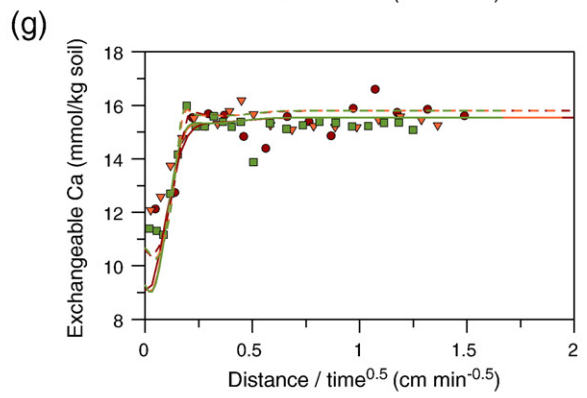
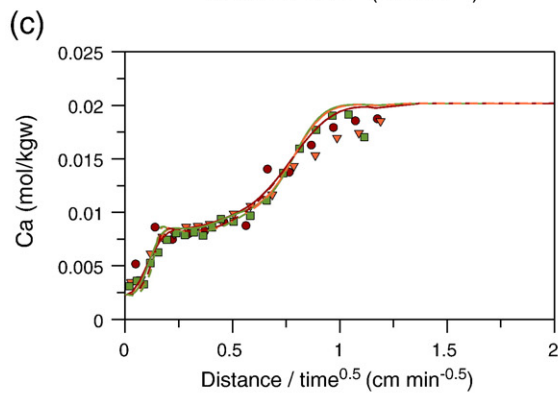
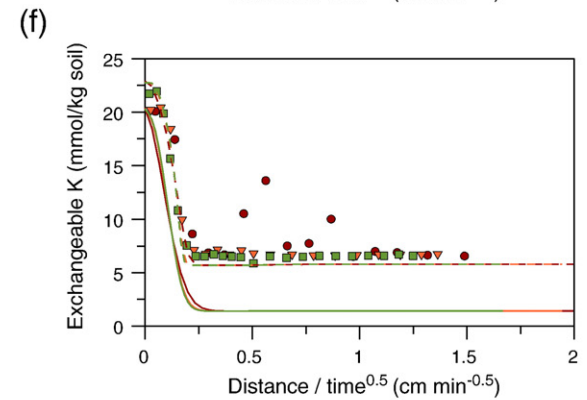
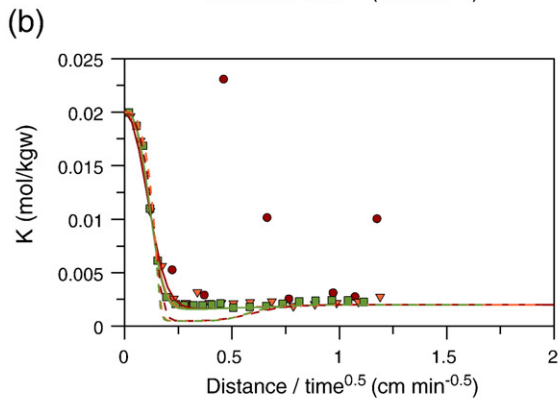
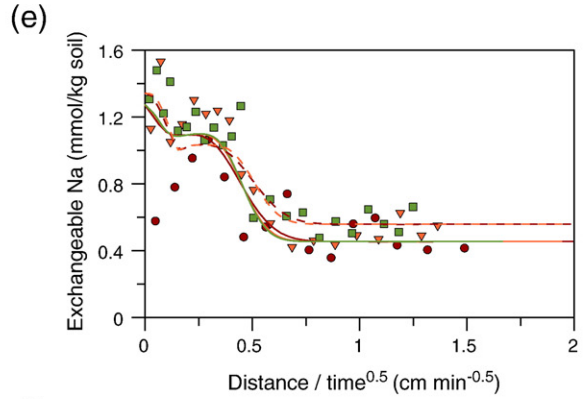
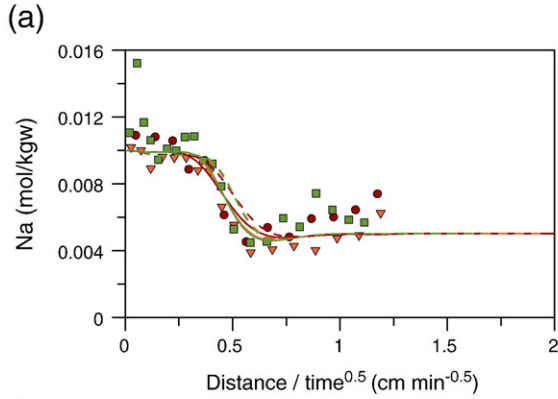


Table 1

Estimated parameter values and linear 95% confidence intervals (CI) for the Gapon approach.

Parameter	Final value	Upper 95% CI	Lower 95% CI	Standard deviation
<i>Optimization with estimated CEC</i>				
Log K_{CK}	0.91	0.96	0.85	0.027
Log K_{Ca}	0.56	0.59	0.53	0.015
Log K_{Mg}	0.16	0.19	0.12	0.018
CEC (mol/dm ³)	0.072	0.073	0.071	5.4×10^{-4}
<i>Optimization with fixed CEC^a</i>				
Log K_{CK}	0.99	1.05	0.93	0.029
Log K_{Ca}	0.56	0.60	0.53	0.016
Log K_{Mg}	0.19	0.22	0.15	0.018

^a The value of CEC was fixed at 0.077 mol/dm³.

displacement of the initial solution. In the region where the Boltzmann variable is smaller than 0.25 cm/min^{0.5}, typical cation exchange reactions occur, during which Na and K replaces Ca and Mg. Since all experimental curves coalesce in this region after applying the Boltzmann transformation, the exchange processes are in chemical equilibrium (i.e., time-scales for chemical reactions are short relative to time-scales of solute movement).

3.1. Optimization results

Fig. 1 compares the water content (θ) and chloride concentration profiles measured during the experiments with the optimized model predictions. Both the Richards equation and the advection–dispersion equation were able to reproduce very well the experimental water content and chloride profiles, respectively. Note that the simulated Cl profiles are a slightly ahead of the experimental data around the piston front. Fitted parameters are $\theta_s = 0.307 \text{ cm}^3 \text{ cm}^{-3}$, $\alpha = 0.230 \text{ cm}^{-1}$, $n = 1.45$, $K_s = 0.157 \text{ cm min}^{-1}$, $l = 0.99$, and $\lambda = 0.0694 \text{ cm}$.

The modeled profiles of the major cations in the aqueous and sorbed phases for the three times are compared to the measured data in Fig. 2. In general, both approaches are able to describe the experimental data reasonably well, although each model missed some particularities of the experimental data.

Fitted parameters are given in Tables 1 and 2 for the Gapon and the Rothmund–Kornfeld approaches, respectively. The weighted sum of squared differences (SSD) is about 20% lower for the Rothmund–Kornfeld approach than for the Gapon approach. The lower SSD for the Rothmund–Kornfeld approach is to be expected, because of the higher number of adjustable parameters in the geochemical model (7 versus 4 in the Gapon approach). Nevertheless, both the Akaike's information criterion (AIC) and the Bayesian information criterion (BIC) (Hill and Tiedeman, 2007) are also lower for the Rothmund–Kornfeld approach (−959 and −926 for AIC and BIC, respectively) than for the Gapon approach (−875

Table 2

Estimated parameter values and linear 95% confidence intervals (CI) for the Rothmund–Kornfeld approach.

Parameter	Final value	Upper 95% CI	Lower 95% CI	Standard deviation
Log K_{RCKNa}	1.14	1.18	1.10	0.010
Log $K_{RCKCaNa}$	1.85	1.98	1.72	0.069
Log $K_{RCKMgNa}$	1.27	1.42	1.12	0.076
N_{KNa}	0.307	0.383	0.230	0.039
N_{CaNa}	0.717	0.784	0.647	0.035
N_{MgNa}	0.843	0.929	0.756	0.044
CEC (mol/dm ³)	0.079	0.081	0.079	7.9×10^{-4}

and −855 for AIC and BIC, respectively). The difference between the two approaches is sufficiently large enough (Burnhum and Anderson, 2004) to give preference to the Rothmund–Kornfeld model. Based on the SSD, AIC, and BIC, the Rothmund–Kornfeld model fits the experimental data better than the Gapon model.

The Gapon approach was additionally used to optimize the exchange constants while setting CEC equal to the measured value (0.077 mol/dm³). Fitted values are again given in Table 1. The aqueous concentrations were almost identical to those obtained when the CEC was optimized. The largest differences were in the initial sorbed Ca and Mg concentrations, which were about 6.5 and 13% higher, respectively, when the CEC was not optimized. However, the 95% confidence intervals of the three exchange parameters obtained using the two approaches (optimized and fixed CEC) overlap.

The fitted CEC was 0.072 and 0.079 mol/dm³ for the Gapon and the Rothmund–Kornfeld approaches, respectively. These values are, respectively, slightly lower and greater than the measured CEC of $0.077 \pm 0.002 \text{ mol/dm}^3$. The linear 95% confidence interval (CI) of the CEC is small, which indicates a well-defined value. Note that the measured CEC falls within the 95% confidence interval of the CEC estimated using the Rothmund–Kornfeld approach, but not the Gapon approach. Correlation coefficients of the CEC with the other parameters are all less than 0.1 in both approaches (Table 3).

The correlation coefficients for other parameters in the Gapon approach were also relatively small, with only one being larger than 0.75 (between log K_{Ca} and log K_{Mg}). Each correlation coefficient between two log K_{GM} was positive (Table 3). The parameters of the Gapon exchange equations, calculated from the fitted half-reaction constants, were: $K_{CaNa} = 3.55$, $K_{CaK} = 0.46$, and $K_{CaMg} = 2.51$. Uncertainty of the estimated parameters was slightly larger in the Rothmund–Kornfeld approach, as evidenced by a greater number of correlation coefficients exceeding 0.75 (Table 4). Further analysis of the identifiability and uniqueness of the fitted parameters is given below using the response surface analysis of the objective function.

The Gapon approach was able to describe Na in the aqueous and exchange phase within the scatter of the

Fig. 2. Simulated profiles of aqueous (a–d) and sorbed (e–h) cation concentrations obtained with the Gapon approach [solid lines] or the Rothmund–Kornfeld approach [dashed lines] compared to experimental data [symbols] from water absorption and solute transport experiments with piggery effluent (Smiles and Smith, 2004b).

Table 3

Correlation coefficients between parameters used in the Gapon approach.

	Log K_{GK}	Log K_{GCa}	Log K_{GMg}	CEC (mol/dm ³)
Log K_{GK}	1			
Log K_{GCa}	0.383	1		
Log K_{GMg}	0.327	0.811	1	
CEC (mol/dm ³)	0.206	6.41×10^{-2}	0.241	1

experimental data. However, the exchangeable K (sorbed) concentration was under-predicted. The description of exchangeable Ca was generally good, with the exception of the final predicted exchangeable Ca when the Boltzmann variable is less than 0.2 cm min^{0.5}. The description of exchangeable Mg was generally within the variability in the experimental data, although close inspection of the aqueous Mg data suggests that the simulated concentration front is slightly ahead of the measured data between the piston front and the region of cation exchange (i.e., between 0.25 and 0.75 cm min^{-0.5}; Fig. 2d). The Gapon approach seemed to be unable to describe sorbed K concentrations, especially when the K concentrations are low and the concentrations of the bivalent cations (in particular Ca) are high (initial condition). Thus, at low K concentrations, sorption is apparently stronger than can be described by the Gapon approach. Although not investigated in detail here, a possible reason for high K sorption at low concentrations may have been the presence of illite in the soil sample (20% of the clay, Smiles and Smith, 2004b). Illite typically has some high-preference sorption sites for K, that are related to the formation of K inner-sphere complexes between the clay surfaces (Evangelou and Philipps, 2005).

As suggested earlier by the weighted sum of squared differences, the Akaike's information criterion, and the Bayesian information criterion, the Rothmund–Kornfeld approach appears to describe the experimental data better than the Gapon approach. While the overall description of the cations' behavior was similar between the Rothmund–Kornfeld and Gapon conventions, the simulated initial and final exchangeable K and Ca more closely matched measured values when using the Rothmund–Kornfeld approach.

Another way of representing the data is to show the sorbed concentrations against the aqueous concentrations (Fig. 3). The redistribution of aqueous Ca and Mg without any visible changes in the cation exchange composition around the piston front is clearly illustrated in this figure (vertical

Table 4

Correlation coefficients between parameters used in the Rothmund–Kornfeld approach.

	Log K_{GK}	Log K_{GCa}	Log K_{GMg}	N_{KNa}	N_{CaNa}	N_{MgNa}	CEC
Log K_{GK}	1						
Log K_{GCa}	0.268	1					
Log K_{GMg}	0.221	0.722	1				
N_{KNa}	-0.422	0.467	0.354	1			
N_{CaNa}	-0.03	-0.926	-0.676	-0.556	1		
N_{MgNa}	-0.01	-0.739	-0.922	-0.478	0.825	1	
CEC	0.580	0.223	0.229	-0.490	-0.178	-0.174	1

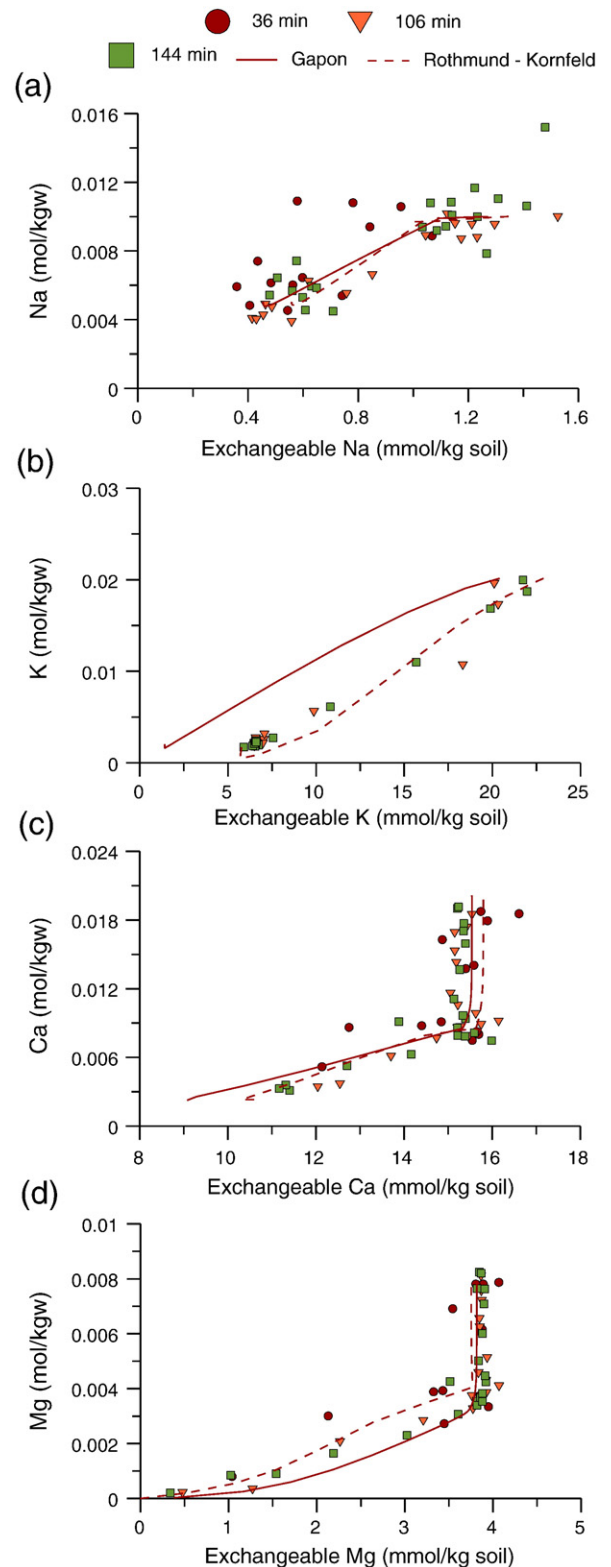


Fig. 3. Simulated relations between sorbed and aqueous concentrations obtained with the Gapon approach [solid lines] or the Rothmund–Kornfeld approach [dashed lines] compared to experimental data [symbols] from water absorption and solute transport experiments with piggy effluent (Smiles and Smith, 2004b).

lines in Fig. 3c, d) and nicely represented by both model approaches. Given the large scatter in the experimental data, it is impossible to make any conclusions about the adequacy of the two models when comparing their results with the Na, Mg, and Ca data. However, the Rothmund–Kornfeld approach performs much better in reproducing the K isotherm than the Gapon approach. At high sorbed (and aqueous) K concentrations, both approaches perform equally well. However, at low K concentrations, sorption in the Rothmund–Kornfeld approach is larger than in the Gapon approach, indicating some preferential sorption of K at low concentrations.

3.2. Information content in experimental data

The composite-scaled sensitivity coefficients (*css*) for the Gapon parameters are given in Table 5. The experimental data contain the most information for the estimation of the cation exchange capacity (CEC), although the *css* for K_{GCa} is also high. Less information is present in the experimental data to estimate K_{GK} and K_{GMg} . The sorbed data provide more information than the aqueous data, as indicated by higher values of the average dimensionless scaled sensitivity coefficients (*dss*) (Table 5), except for K. From the four cations, Ca has the largest average dimensionless scaled sensitivity.

In many cases, identifiability of a particular parameter benefits from a combination of different data types, because a single parameter influences multiple output variables. In addition, the dimensionless scaled sensitivities change with observations as a function of the Boltzmann variable. Let us provide interpretation of *dss* for K_{GCa} , which has high values for aqueous Na and K concentrations around their moving fronts and for sorbed Ca concentrations (Fig. 4). While the Na front with increasing aqueous Na concentrations passes close behind the piston front, the K front, where K replaces Ca and Mg on the exchange sites, is nearer to the inlet boundary. Higher K_{GCa} will result in less K on the exchange complex, which explains the high *dss* for aqueous K between 0.25 and 0.75 cm/min^{0.5}. Similarly, a higher K_{GCa} will result in more Na in the aqueous phase, which explains the high *dss* for aqueous Na concentrations. Also, the value of K_{GCa} defines the amount of the sorbed Ca, which explains the high *css* for

the sorbed Ca for the whole profile. All other *dss* profiles can be interpreted in a similar way.

This information content is similar for all aqueous data. Aqueous concentrations do not contribute to the information content ahead of the piston flow (i.e., for the Boltzmann variable larger than 0.75 cm/min^{0.5}) where *dss* is close to zero. Aqueous Na concentrations provide useful information between 0.25 and 0.75 cm/min^{0.5} where the Na front is located. The three other cations provide the most information around the K front where sorbed K replaces sorbed Ca and Mg (between 0 and 0.25 cm/min^{0.5}). On the other hand, the information content of the sorbed concentrations is quite independent of the Boltzmann variable, at least when it is larger than 0.25 cm/min^{0.5}, since in this region there are no changes in sorbed concentrations of K, Ca, and Mg. However, the initial sorbed concentrations (especially Ca and Mg) have important information for several parameters because they constrain the initial distribution of cations between aqueous and sorbed concentrations. Additional information is contained in sorbed concentrations at the inlet where the exchange between K, Ca, and Mg is complete (i.e., at small Boltzmann variables). Additionally, the concentration profiles measured at 144 min provide more information than the other two datasets since they contain more data points with higher sensitivity.

A similar analysis was also done for the Rothmund–Kornfeld approach (Table 6 and Fig. 5). The *css* values for the Rothmund–Kornfeld approach are larger than those for the Gapon approach. In fact, *css* of the parameters involving K exchange are smaller compared to those of the other parameters. The profiles of the dimensionless scaled sensitivities of the observations for K_{RKKNa} , K_{RKCNa} , K_{RKMgNa} , and the CEC (results not shown) are very similar to those for the Gapon approach, except that they have higher absolute values. For the *N* coefficients in the Rothmund–Kornfeld approach, sorbed Ca and Mg concentrations are the most informative experimental data ahead of the piston front. For Boltzmann variables smaller than 0.25 cm/min^{0.5}, the aqueous Ca and Mg concentrations provide similar amount of information compared to the sorbed Ca and Mg concentrations. As expected from the *css* of N_{KNa} , the dimensionless scaled sensitivity for this parameter is small.

Table 5

Composite-scaled sensitivities (*css*, top value in the second column), percentage of *css* compared to maximum values (bottom value in the second column) and the averaged dimensionless scaled sensitivities (*dss*) for each measured cation for both the aqueous data (top value of columns 3–6) and sorbed data (bottom value of columns 3–6) for the Gapon approach.

Parameter	<i>css</i>	Na	K	Ca	Mg
Top value	(Absolute value)	(Aqueous)	(Aqueous)	(Aqueous)	(Aqueous)
Bottom value	(% of max)	(Sorbed)	(Sorbed)	(Sorbed)	(Sorbed)
Log K_{GK}	0.65	0.222	0.504	0.241	0.095
	0.27	0.300	0.425	0.679	0.187
Log K_{GCa}	1.11	0.357	0.266	0.119	0.222
	0.46	0.709	0.213	1.822	1.814
Log K_{GMg}	0.25	0.023	0.011	0.030	0.039
	0.10	0.124	0.012	0.387	0.538
CEC (mol/dm ³)	2.4	0.374	0.423	0.226	0.197
	1.00	0.768	0.289	5.916	1.870

Bold values indicate the experimental dataset which provides the largest information for a given parameter.

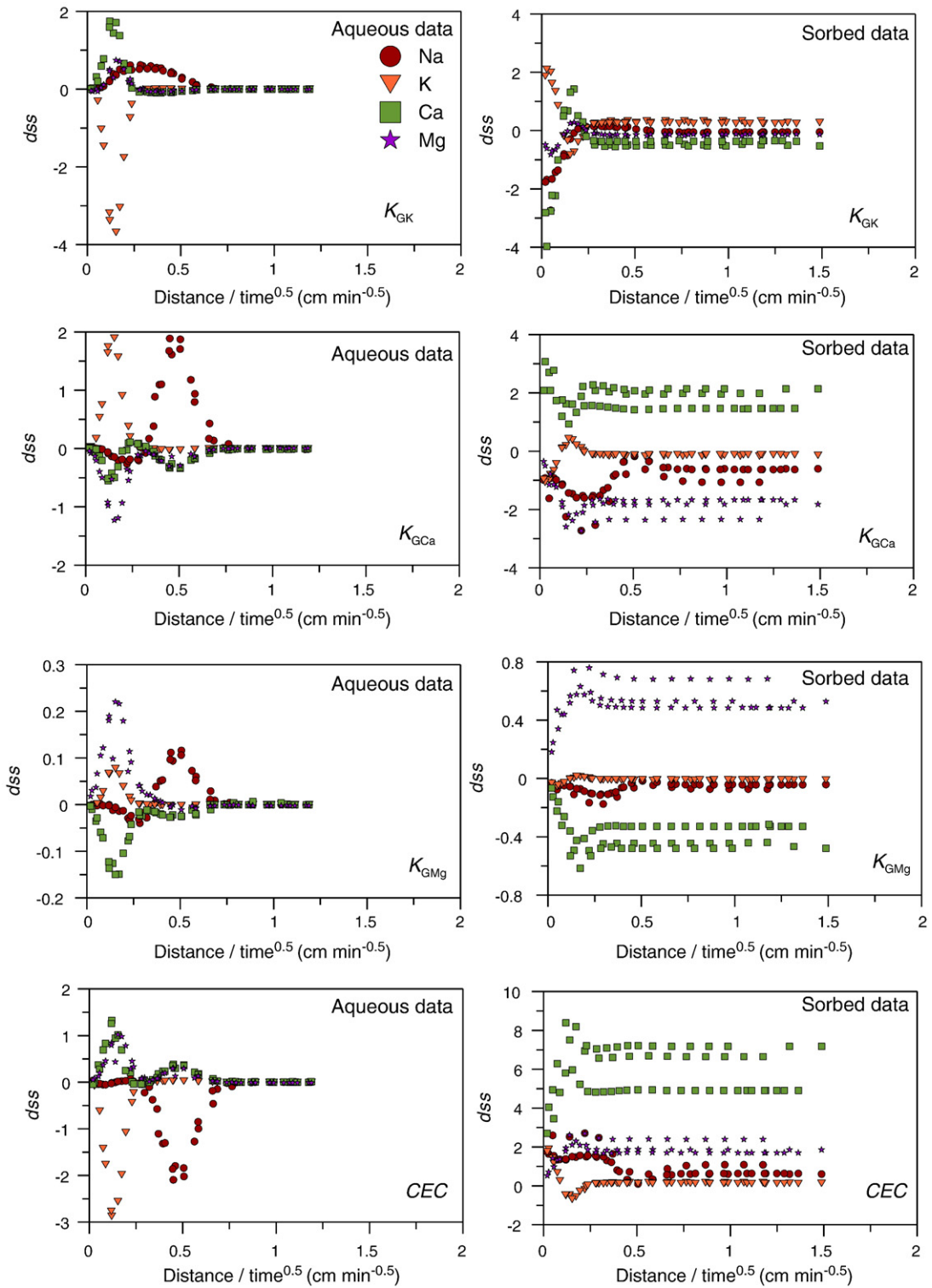


Fig. 4. Profiles of dimensionless-scaled sensitivities (dss) for the parameters in the Gapon approach for the aqueous (left) and sorbed (right) data.

The above discussed information content can be used when designing the experimental set up and procedures. The highest information content is in, and thus it should be

desirable to measure, initial sorbed concentrations and aqueous concentrations of different cations at different critical positions behind the piston front (i.e., around the Na

Table 6

Composite-scaled sensitivities (*css*, top value in the second column), percentage of *css* compared to maximum values (bottom value in the second column) and the averaged dimensionless scaled sensitivities for each measured cation for both the aqueous data (top value of columns 3–6) and sorbed data (bottom value of columns 3–6) for the Rothmund–Kornfeld approach.

Parameter	<i>css</i>	Na	K	Ca	Mg
Top value	(Absolute value)	(Aqueous)	(Aqueous)	(Aqueous)	(Aqueous)
Bottom value	(% of max)	(Sorbed)	(Sorbed)	(Sorbed)	(Sorbed)
Log K_{RKNa}	1.44	0.315	0.692	0.396	0.173
	0.41	0.403	1.449	2.273	0.722
Log K_{RKCNa}	3.48	0.482	0.637	0.269	0.600
	1.00	1.251	0.999	6.386	5.838
Log K_{RKMgNa}	2.04	0.061	0.051	0.174	0.348
	0.58	0.282	0.122	3.064	4.349
N_{KNa}	0.22	0.045	0.200	0.094	0.052
	0.06	0.172	0.177	0.285	0.093
N_{CaNa}	3.46	0.216	0.301	0.470	1.128
	0.99	1.094	0.849	6.414	5.925
N_{MgNa}	3.08	0.072	0.127	0.545	1.201
	0.88	0.318	0.202	4.514	6.393
CEC (mol/dm ³)	2.47	0.320	0.486	0.247	0.219
	0.71	0.863	0.662	5.900	1.879

Bold values indicate the experimental dataset which provides the largest information for a given parameter.

front and around the K front when K displaces Ca and Mg on the exchange sites). In general, the measurement of a single profile at a large time should be sufficient because such measurement provides more informative data points.

3.3. Response surface analysis of the objective function

Two-dimensional contour plots of the objective function can be used to investigate the identifiability of optimized parameters and their mutual correlations. In the soil hydrological literature, contour plots are often used to investigate the identifiability, uncertainty, and correlation of soil hydraulic parameters in an inverse optimization problem (e.g., Šimůnek and van Genuchten, 1996; Toorman et al., 1992). Such analysis often indicated that many soil hydraulic parameters are not well defined or strongly correlated. For example, for the one-step outflow experiment, Toorman et al. (1992) identified close correlations between parameters α - n and α - K_s . Similarly, Šimůnek and van Genuchten (1996) found close correlations between parameters α - n , α - K_s , and n - K_s for the tension disk infiltration experiment. In both of these experiments, only water flux was measured, and the parameter identifiability dramatically improved when additional information (such as pressure heads) was provided. The severity of unidentifiability or correlation thus depends strongly on the boundary conditions applied and/or the measured variables (e.g., water contents, water fluxes, pressure heads) used to constrain the inverse optimization.

Fig. 6 shows three selected contour plots (out of six) for the parameters in the Gapon approach. Well identifiable parameters show a well-defined single minimum (i.e., a small circular region). For example, parameter uncertainty and correlations are small in the $\log K_{\text{GK}}$ - $\log K_{\text{GCa}}$ (Fig. 6a) and $\log K_{\text{GK}}$ -CEC (Fig. 6c) planes. Less-identifiable parameters show contour plots with an extended region around the minimum or multiple minima, indicating that the same value of the objective function can be obtained for different

combinations of optimized parameters (e.g., the $\log K_{\text{GC}}$ - $\log K_{\text{GMg}}$ contour plot, Fig. 6b). Extended regions of small values of the objective function indicate an increased uncertainty of optimized parameters. Overall, Fig. 6 shows that the experimental set-up used in this study permits the estimation of well-defined reaction parameters, which is in contrast to many experimental setups used for determining soil hydraulic parameters.

The same analysis was also performed also for the parameters of the Rothmund–Kornfeld approach. The analysis for seven parameters results in 21 contour plots, nine of which are shown in Fig. 7. Contour plots not involving N_{KNa} have a well-defined minimum, although a strong correlation exists between two parameters (e.g., between K_{RKCNa} and K_{RKMgNa} or between K_{RKCNa} and N_{CaNa} , as previously discussed). The contour plots with N_{KNa} show contours parallel with the N_{KNa} axis, which indicates that N_{KNa} is a rather insensitive parameter (as was also clear from the analysis of *css* and the dimensionless scaled sensitivity values). Nevertheless, although N_{KNa} itself is a rather insensitive parameter, there is a significant improvement in applying the Rothmund–Kornfeld approach rather than the Gapon approach to the K isotherm (Fig. 3). Although the analysis of the sensitivities (discussed above) indicated that the experimental data contained significant information to estimate the Rothmund–Kornfeld parameters, the two-dimensional contour analysis shows that some parameters are ill-defined.

3.4. Validation of derived parameters

In the present experiment, the main interest was in estimating the cation exchange parameters. Soil hydraulic and solute transport parameters were fitted in order to have a proper description of the water flow and hydrodynamic dispersion processes, thus removing confounding effects from the results. The fitted hydraulic and solute transport parameters, which are often affected by the soil structure, are

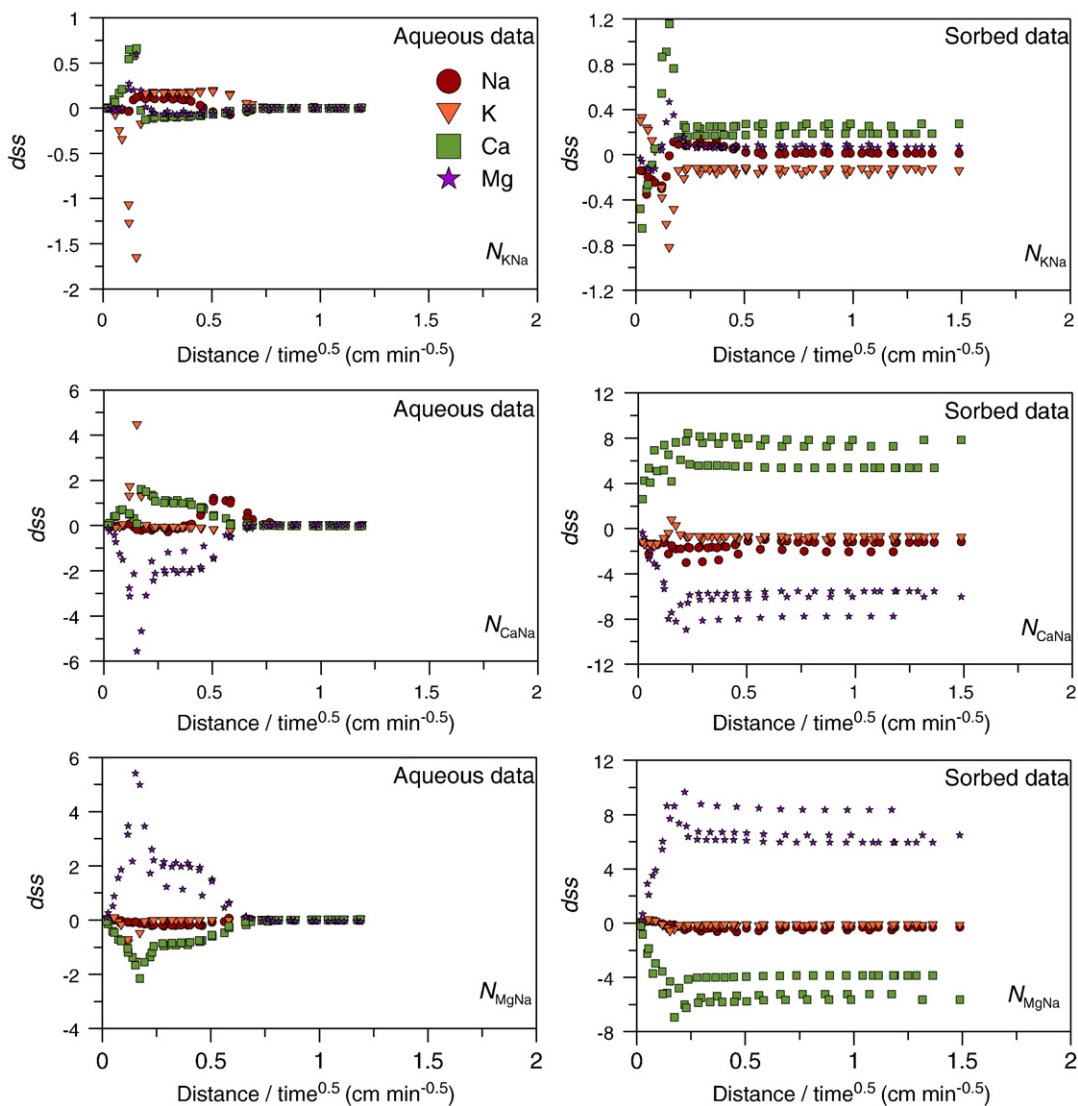


Fig. 5. Profiles of dimensionless-scaled sensitivities (dss) for selected parameters in the Rothmund–Kornfeld approach for the aqueous (left) and sorbed (right) data.

of minimal relevance to similar but undisturbed field soil because the laboratory experiments were carried out using a highly disturbed soil material. In contrast, cation exchange parameters estimated using the disturbed soil are assumed to be applicable to other disturbed and undisturbed soils of the same type and chemical composition, since these parameters are affected mainly by the soil texture and mineralogy. This hypothesis was tested by applying the cation exchange parameters derived from experimental data of Smiles and Smith (2004b) against a new experimental dataset (Smiles and Smith, 2008) that uses the same soil, with the exception that it had been irrigated with K-rich effluent. In this experiment, water equilibrated with gypsum was absorbed into a soil column that initially had a high exchangeable K ratio (Smiles and Smith, 2008).

The performance of the model and its optimized parameters were evaluated by comparing calculated and measured

concentration profiles for major cations in the aqueous phase and on the exchange sites (Fig. 8). The larger differences between the initial sorbed measured and simulated concentration compared to the differences between the initial aqueous measured and simulated concentrations are because the initial sorbed concentrations are calculated with the geochemical model, whereas the measured initial aqueous concentrations are direct input in the model. The calculated aqueous concentrations of Na, K, Ca, and Mg agree well with the measured data when the Gapon coefficients are used. In contrast, there were larger variations between the measured and calculated data using the Rothmund–Kornfeld approach. In general, the Gapon exchange convention provides better agreement between the simulated and measured data compared to the Rothmund–Kornfeld convention. Although the Rothmund–Kornfeld approach fitted the first set of experiments better (considering the Akaike criterion), a

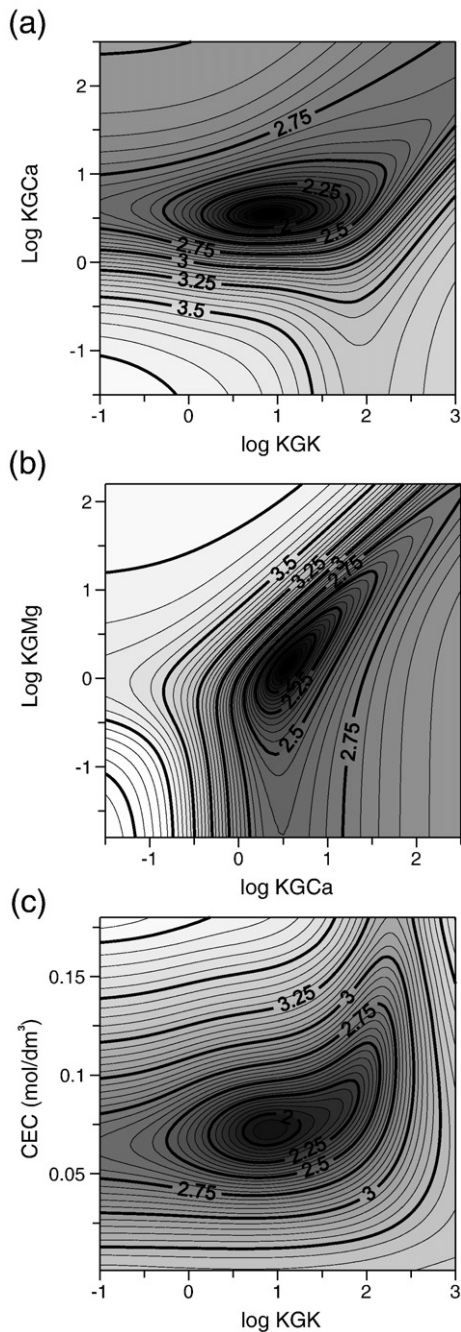


Fig. 6. Contour plots of the objective function defined using the aqueous and sorbed concentrations for the Gapon approach. (a) $\log KGK$ – $\log KGCa$, (b) $\log KGCa$ – $\log KGMg$, and (c) $\log KGK$ – CEC .

larger number of optimized parameters led to higher uncertainty and lower identifiability, as was shown using the analysis of the dimensionless scaled sensitivity coefficients and response surfaces. That is, the Rothmund–Kornfeld model is slightly over-parameterized given the experimental information content. This means that some optimized parameters may not have physical meaning and may not be reliable when used in conditions other than those for which

they were calibrated. The Gapon convention, which uses fewer parameters, appears to be more robust.

Three different analyses discussed above (i.e., information content analysis, response surfaces analysis, and validation) showed that under conditions involving the transport of multiple cations (i.e., Na, K, Ca, and Mg), the aqueous and sorbed concentrations are not sensitive to the N_{KNa} parameter of the monovalent exchange reaction. Predicted concentrations are more sensitive to parameters describing the heterovalent exchange. However, PHREEQC calculations of binary monovalent exchange between K and Na showed that the K-isotherm in particular is quite sensitive to N_{KNa} (results not shown). It may be worthwhile to investigate if the inverse problem for the Rothmund–Kornfeld approach would be better defined when independent measurements of binary monovalent exchange for the K-isotherm (covering the entire range of the sorbed mole fraction) are included.

4. Summary and conclusions

Previously published laboratory experiments by Smiles and Smith (2004b) that examined the transport of major ions during water absorption in horizontal soil columns were used here to estimate soil hydraulic, solute transport, and solute reaction parameters. Soil hydraulic parameters were estimated first using the measured water content profiles at three different times with the inverse option of HYDRUS-1D. Solute transport parameters were then similarly identified using the measured Cl profiles. Finally, the geochemical parameters of the cation exchange were estimated using liquid-phase and exchange-phase concentrations of four major cations (Na, K, Mg, and Ca), the biogeochemical HP1 code, and the universal optimization code, UCODE. The cation exchange parameters were identified for the Gapon and Rothmund–Kornfeld models. While both approaches described the experimental data reasonably well, the Rothmund–Kornfeld model described the experimental data better than the Gapon model during the calibration stage. Both the Akaike's information criterion and the Bayesian information criterion indicated that, despite having more parameters and consequently providing more flexibility in fitting experimental data than the Gapon model, the Rothmund–Kornfeld model was superior.

The information content and response surface analyses indicated that while all parameters of the Gapon model were well identifiable, there was a close correlation between several parameters of the Rothmund–Kornfeld model (Figs. 6 and 7). Thus, using the Rothmund–Kornfeld convention, these parameters cannot be identified simultaneously from the experimental data and some need to be measured, or otherwise estimated, independently.

These findings were confirmed by a subsequent validation exercise, in which geochemical reaction parameters estimated from the initial set of column experiments were used to predict liquid-phase and exchange-phase concentrations of four major cations from another set of experiments involving absorption of gypsum-saturated water into horizontal soil columns. While the parameters of the Gapon model allowed for a good fit between the modeled and empirical aqueous data, the parameters of the Rothmund–Kornfeld model resulted in a poorer fit, attributed to the fact that not all

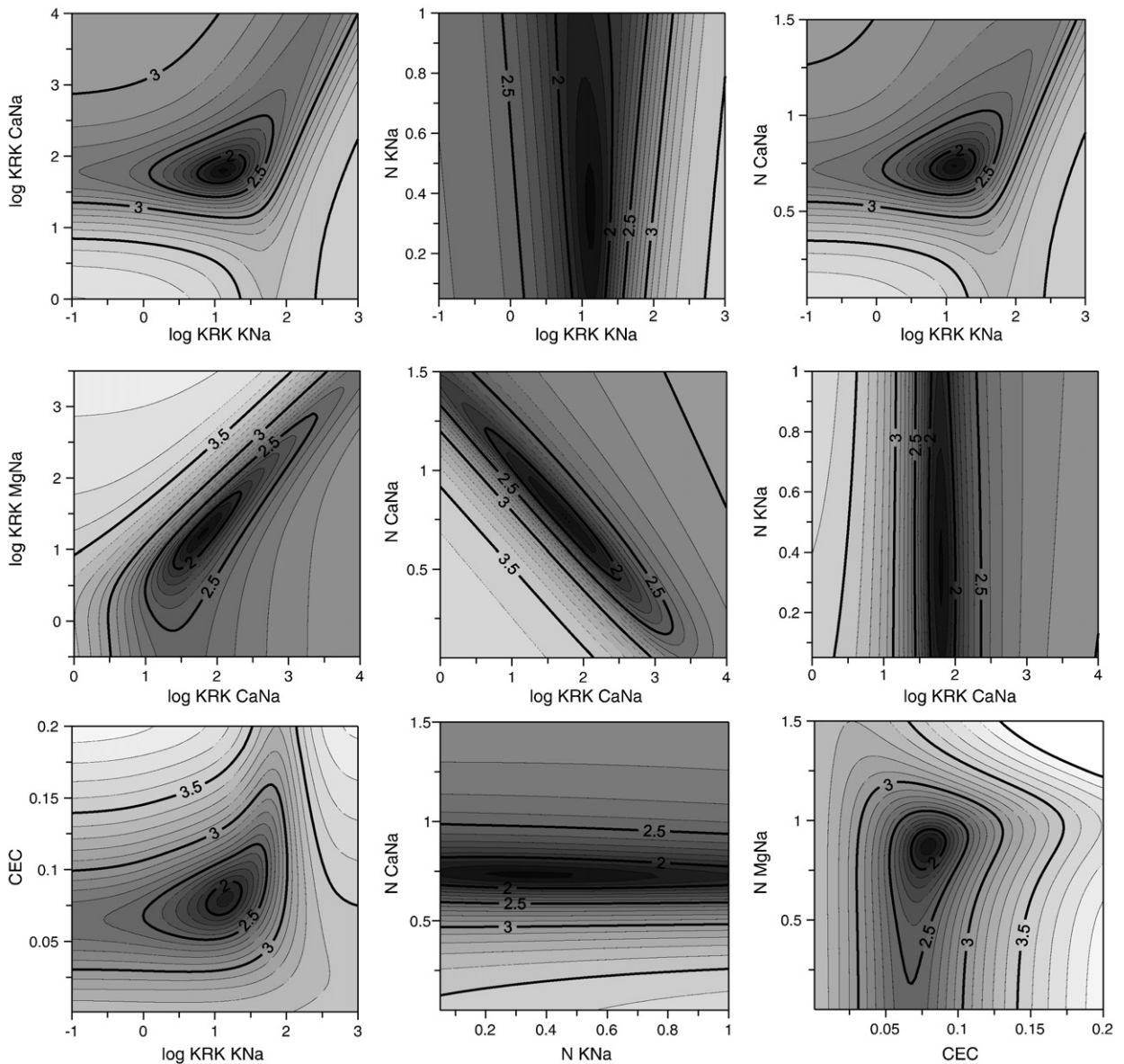


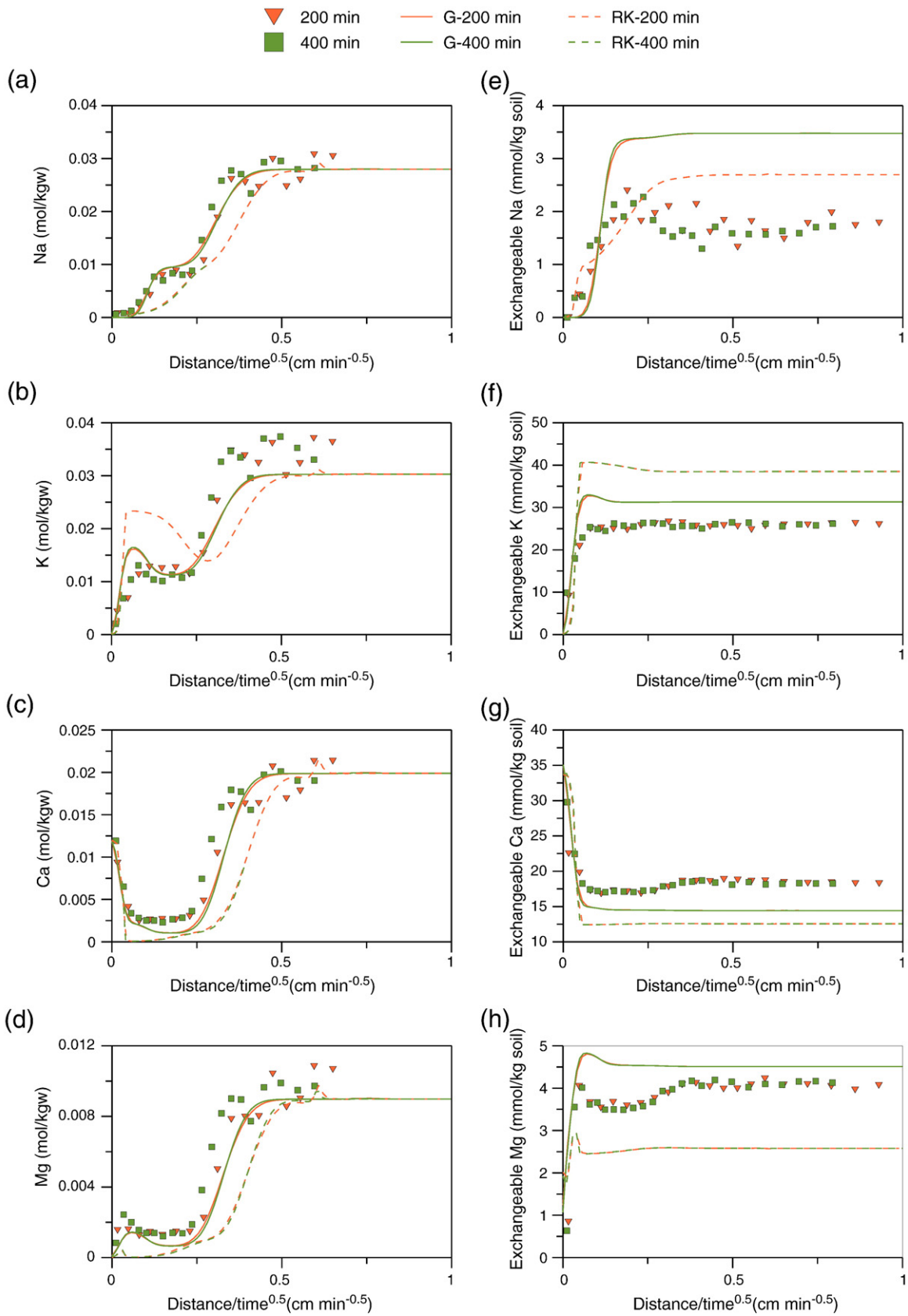
Fig. 7. Contour plots of the objective function defined using the aqueous and sorbed concentrations for the Rothmund–Kornfeld approach. First column: (top) $\log K_K - \log K_{Ca}$, (middle) $\log K_{Ca} - \log K_{Mg}$, and (bottom) $\log K_K - \text{CEC}$; Second column: $\log K_K - n_K$, $\log K_{Ca} - n_{Ca}$, and $\log K_K - n_{Ca}$; Third column: $\log K_K - n_{Ca}$, $\log K_{Ca} - n_K$, and $\log K_K - n_{Mg}$.

parameters were identifiable, as shown by the analysis of the information content and response surfaces.

The combined use of the flow and transport code HYDRUS-1D, the biogeochemical code HP1, and the universal optimization code UCODE proved to be a powerful tool for analyzing experimental data involving transient variably-saturated water flow, solute transport, and geochemical reactions. A flexible code, such as HP1, allows one to analyze

different geochemical conceptual models (in our case, the Gapon and Rothmund–Kornfeld models) using one code. A key element however, is that experimental data should contain enough information to estimate all parameters. For example, the sensitivity analysis indicated that the current experimental data (Smiles and Smith, 2004b) does not contain enough information to identify all parameters in the Rothmund–Kornfeld model.

Fig. 8. Experimental [symbols] and simulated [solid lines for the Gapon approach and dashed lines for the Rothmund–Kornfeld approach] profiles of water soluble and exchangeable cations during the absorption of gypsum-saturated solution into a soil column.



Appendix 1

1. A section of the HP1 input file where the cation exchange is defined using the Gapon convention:

```
EXCHANGE_MASTER_SPECIES
  GG-
EXCHANGE_SPECIES
  G-=G-; log_k 0
  G-+Na+=NaG; log_k 0
  G-+K+=KG; log_k 1.16
  G-+0.5 Ca+2=Ca0.5G; log_k 0.462
  G-+0.5 Mg+2=Mg0.5G; log_k 0.383.
```

Where \log_k is $\log K$ of the reaction (values given here are the initial estimates). The reference half-reaction for each exchanger is Na; the half reaction is $\text{Na}^+ + \text{X}^- = \text{NaX}$ and it has a $\log K$ of 0.0.

2. A section of the HP1 input file where the cation exchange is defined using the Rothmund–Kornfeld equations:

```
EXCHANGE_MASTER_SPECIES
  RR-
EXCHANGE_SPECIES
  R-=R-; log_k 0
  Na++R-=NaR; log_k 0
  0.318 K++NaR=KR+.318 Na+; log_k 1.12;
-no_check; -mole_balance KR
  0.736 Ca+2+2NaR=CaR2+1.472Na+; log_k
1.804; -no_check; -mole_balance CaR2
  0.868 Mg+2+2NaR=MgR2+1.712 Na+; log_k 1.224;
-no_check; -mole_balance MgR2.
```

References

- Appelo, C.A.J., Postma, D., 2005. *Geochemistry, Groundwater and Pollution*, 2nd ed. AA Balkema Publishers, Leiden. The Netherlands a member of Taylor & Francis Group plc.
- Bloom, S.A., Mansell, R.S., 2001. An algorithm for generating cation exchange isotherms from binary selectivity coefficients. *Soil Science Society of America Journal* 65, 1426–1429.
- Bond, W.J., 1995. On the Rothmund–Kornfeld description of cation exchange. *Soil Science Society of America Journal* 59, 436–443.
- Bond, W.J., 1997. Competitive exchange of K^+ , Na^+ and Ca^{2+} during transport through soil. *Australian Journal of Soil Research* 35, 739–752.
- Bond, W.J., Phillips, I.R., 1990a. Cation exchange isotherms obtained with batch and miscible-displacement techniques. *Soil Science Society of America Journal* 54, 722–728.
- Bond, W.J., Phillips, I.R., 1990b. Approximate solutions for cation transport during unsteady, unsaturated soil water flow. *Water Resources Research* 26, 2195–2205.
- Bond, W.J., Verburg, K., 1997. Comparison of methods for predicting ternary exchange from binary isotherms. *Soil Science Society of America Journal* 61, 444–455.
- Burnham, K.P., Anderson, D.R., 2004. Multimodal inference: understanding AIC and BIC in model selection. *Sociological Methods & Research* 33, 261–304.
- Clausnitzer, V., Hopmans, J.W., 1995. Non-linear parameter estimation: LM_OPT. General purpose optimization code based on the Levenberg–Marquardt algorithm. Land, Air and Water Resources Paper No. 100032. University of California Davis, CA.
- Dai, Z., Samper, J., 2004. Inverse problem of multicomponent reactive chemical transport in porous media: formulation and applications. *Water Resources Research* 40, W07407. doi:10.1029/2004WR003248.
- Evangeliou, V.P., Philipps, R.E., 2005. Cation exchange in soils. In: Tabatabai, M.A., Sparks, D.L. (Eds.), *Chemical Processes in Soil*. Soil Science Society of America, pp. 343–410.
- Friedel, M.J., 2005. Coupled inverse modeling of vadose zone water, heat, and solute transport: calibration constraints, parameter nonuniqueness, and predictive uncertainty. *Journal of Hydrology* 312, 148–175.
- Gonçalves, M.C., Šimůnek, J., Ramos, T.B., Martins, J.C., Neves, M.J., Pires, F.P., 2006. Multicomponent solute transport in soil lysimeters irrigated with waters of different quality. *Water Resources Research* 42, W08401. doi:10.1029/2006WR004802, 17 pp.
- Hill, M.C., Tiedeman, C.R., 2007. *Effective Groundwater Model Calibration with Analysis of Data, Sensitivities, Predictions and Uncertainty*. John Wiley & Sons, NJ, USA.
- Hopmans, J.W., Šimůnek, J., Romano, N., Durner, W., 2002. Inverse modeling of transient water flow. In: Dane, J.H., Topp, G.C. (Eds.), *Methods of Soil Analysis, Part 1, Physical Methods*, Chapter 3.6.2, Third ed. SSSA, Madison, WI, pp. 963–1008.
- Hutson, J.L., Wagenet, R.J., 1992. LEACHM. A process based model of water and solute movement, transformations, plant uptake and chemical reactions in the unsaturated zone. Version 3. Cornell University Department of Soil, Crop and Atmospheric Sciences Research Series No. 92-3.
- Jacques, D., Šimůnek, J., van Genuchten, M.Th., Mallants, D., 2006. Operator-splitting errors in coupled reactive transport codes for transient variably saturated flow and contaminant transport in layered soil profiles. *Journal of Contaminant Hydrology* 88, 197–218.
- Jacques, D., Šimůnek, J., Mallants, D., van Genuchten, M.Th., 2008a. Coupling hydrological and chemical processes in the vadose zone: a case study on long term uranium migration following mineral P-fertilization. *Vadose Zone Journal* 7, 698–711.
- Jacques, D., Šimůnek, J., Mallants, D., van Genuchten, M.Th., 2008b. Modelling coupled water flow, solute transport and geochemical reactions affecting heavy metal migration in a podzol soil. *Geoderma* 145, 449–461.
- Mansell, R.S., Bloom, S.A., Bond, W.J., 1993. Simulating cation transport during water flow in soil: two approaches. *Soil Science Society of America Journal* 57, 3–9.
- Marquardt, D.W., 1963. An algorithm for least-squares estimation of nonlinear parameters. *SIAM Journal on Applied Mathematics* 11, 431–441.
- MDH Engineered Solutions Corp., 2003. Evaluation of computer models for predicting the fate and transport of salt in soil and groundwater. Phase II Report.
- Millington, R.J., Quirk, J.M., 1961. Permeability of porous solids. *Transactions of the Faraday Society* 57, 1200–1207.
- Nkedi-Kizza, P., Biggar, J.W., Selim, H.M., van Genuchten, M.Th., Wierenga, P.J., Davidson, J.M., Nielsen, D.R., 1984. On the equivalence of two conceptual models for describing ion exchange during transport through an aggregated oxisol. *Water Resources Research* 20, 1123–1130.
- Parkhurst, D.L., Appelo, C.A.J., 1999. User's guide to PHREEQC (version 2)—a computer program for speciation, batch-reaction, one-dimensional transport and inverse geochemical calculations. *Water Resources Investigation, Report 99-4259*, Denver, CO, USA.
- Phillips, I.R., Bond, W.J., 1989. Extraction procedure for determining solution and exchange ions in the same soil sample. *Soil Science Society of America Journal* 53, 1294–1297.
- Poeter, E.P., Hill, M.C., Banta, E.R., Mehl, S., Steen, C., 2005. UCODE_2005 and six other computer codes for universal sensitivity analysis, calibration and uncertainty evaluation. *U.S. Geological Survey Techniques and Methods* 6-A11.
- Ramos, T.B., Šimůnek, J., Gonçalves, M.C., Martins, J.C., Prazeres, A., Castanheira, N.L., Pereira, L.S., 2011. Field evaluation of a multicomponent solute transport model in soils irrigated with saline waters. *Journal of Hydrology* 407 (1–4), 129–144 2011.
- Rayment, G.E., Higginson, F.R., 1992. *Australian Laboratory Handbook of Soil and Water Chemical Methods*. Inkata Press, Melbourne.
- Šimůnek, J., van Genuchten, M.Th., 1996. Estimating unsaturated soil hydraulic properties from tension disc infiltrometer data by numerical inversion. *Water Resources Research* 32, 2683–2696.
- Šimůnek, J., Jacques, D., Hopmans, J.W., Inoue, M., Flury, M., van Genuchten, M.Th., 2002. Solute transport during variably-saturated flow—inverse methods. In: Dane, J.H., Topp, G.C. (Eds.), *Methods of Soil Analysis, Part 1, Physical Methods*, Chapter 6.6, Third ed. SSSA, Madison, WI, pp. 1435–1449.
- Šimůnek, J., Jacques, D., van Genuchten, M.Th., Mallants, D., 2006. Multicomponent geochemical transport modeling using HYDRUS-1D and HP1. *Journal of the American Water Research Association* 46, 1537–1547.
- Šimůnek, J., Šejna, M., Saito, H., Sakai, M., van Genuchten, M.Th., 2008a. The Hydrus-1D Software Package for Simulating the One-dimensional Movement of Water, Heat, and Multiple Solutes in Variably-saturated Media. Department of Environmental Sciences, University of California Riverside, Riverside, California.
- Šimůnek, J., van Genuchten, M.Th., Šejna, M., 2008b. Development and applications of the HYDRUS and STANMOD software packages, and related codes. *Vadose Zone Journal*. doi:10.2136/VZJ2007.0077, Special Issue “Vadose Zone Modeling”, 7, 587–600.

- Šimůnek, J., Jacques, D., Twarakavi, N.K.C., van Genuchten, M.Th., 2009. Selected HYDRUS modules for modeling subsurface flow and contaminant transport as influenced by biological processes at various scales. *Biologia* 64, 465–469.
- Smiles, D.E., Smith, C.J., 2004a. A survey of the cation content of piggery effluents and some chemical consequences of their use to irrigate soils. *Australian Journal of Soil Research* 42, 231–246.
- Smiles, D.E., Smith, C.J., 2004b. Absorption of artificial piggery effluent by soil: a laboratory study. *Australian Journal of Soil Research* 42, 96–975.
- Smiles, D.E., Smith, C.J., 2008. Absorption of gypsum solution by a potassic soil: a data set. *Australian Journal of Soil Research* 46, 67–75.
- Toorman, A.F., Wierenga, P.J., Hills, R.G., 1992. Parameter estimation of hydraulic properties from one-step outflow data. *Water Resources Research* 28, 3021–3028.
- Toride, N., Leij, F.J., van Genuchten, M.Th., 1995. The CXTFIT code for estimating transport parameters from laboratory or field tracer experiments. Version 2.0, Research Report No. 137. U. S. Salinity Laboratory, USDA, ARS, Riverside, CA.
- van Genuchten, M.Th., 1980. A closed-form equation for predicting the hydraulic conductivity of unsaturated soils. *Soil Science Society of America Journal* 44, 892–898.
- Voegelin, A., Vulava, V.M., Kuhnlen, F., Kretzschmar, R., 2000. Multicomponent transport of major cations predicted from binary adsorption experiments. *Journal of Contaminant Hydrology* 46, 319–338.
- Voegelin, A., Vulava, V.M., Kretzschmar, R., 2001. Reaction-based model describing competitive sorption and transport of Cd, Zn and Ni in an acidic soil. *Environmental Science & Technology* 35, 1651–1657.
- Vrugt, J.A., Stauffer, P.H., Wöhling, T., Robinson, B.A., Vesselinov, V.V., 2008. Inverse modeling of subsurface flow and transport properties: a review with new developments. *Vadose Zone Journal* 7, 843–864.
- Vulava, V.M., Kretzschmar, R., Rusch, U., Grolimund, D., Westall, J.C., Borkovec, M., 2000. Cation competition in a natural subsurface material: modelling of sorption equilibria. *Environmental Science & Technology* 34, 2149–2155.